In Situ Measurement of Wall Thermal Properties: Parametric Investigation of the Heat Flow Methods Through Virtual Experiments Data

Andrea Alongi – Politecnico di Milano, Italy – andrea.alongi@polimi.it
Luca Sala – Politecnico di Milano, Italy – luca11.sala@mail.polimi.it
Adriana Angelotti – Politecnico di Milano, Italy – adriana.angelotti@polimi.it
Livio Mazzarella – Politecnico di Milano, Italy – livio.mazzarella@polimi.it

Abstract

Energy retrofit of existing buildings is based on the assessment of the starting performance of the envelope. The procedure to evaluate thermal conductance through in situ measurements is described in the technical standard ISO 9869-1:2014, which provides two alternative techniques to process collected data: the Average Method (AM) and the Dynamic Method (DM).

This work studies their effectiveness using virtual data from numerical simulations of three kinds of walls, performed using a Finite Difference model.

The AM always provides acceptable estimates in winter, with better outcomes when indoor heat flux is considered in every case except the highly insulated wall. Summer conditions do not lead to acceptable measurements, despite the fulfillment of the check required by the standard. The DM results show acceptable estimations of the thermal conductance in both climates, for most of the virtual samples considered, although critically depending on some parameters of the DM that are left to the user's discretion, without strict indications by the standard. This work highlights a possible approach for overcoming this issue, which requires deeper future investigation.

1. Introduction

To reduce the energy needs related to the existing building stock, great effort is oriented towards envelope renovation. As a first step in this direction, the thermal properties (thermal transmittance and conductance) of the existing building components are usually assessed through in situ measurements. To this purpose, the international technical standard ISO 9869-1:2014 describes the so-called Heat Flow

Meter method and two data processing techniques: the Average and the Dynamic Method.

Within the dedicated literature there is a wide variety of results (Atsonios et al., 2017; Gaspar et al., 2018; Lucchi et al., 2017). This is possibly due to the diversity of wall typologies investigated and boundary conditions occurring. Moreover, even when different walls are studied in the same work (Atsonios et al., 2017), experimental measurements are not performed at the same time.

To overcome the limitations inherent with experimental approaches, this work analyzes the efficacy of the Average and the Dynamic Method in finding the wall conductance by using virtual wall samples with different known properties, simulated through a Finite Difference model with controlled and repeatable boundary conditions. Moreover, these analyses are also aimed at looking for supplementary criteria concerning some key parameters of each methodology.

2. Methods and Materials

In this paper the Average and the Dynamic methods of analysis suggested by ISO 9869-1:2014 are applied to virtual data obtained through virtual Heat Flow Meter experiments i.e., heat transfer numerical simulations on wall components. The purpose of the data analysis is to derive the "experimental" thermal conductance, that in this case can be compared with the exactly known true value. In this section the experimental and data processing approaches by the standard are briefly illustrated. Secondly, the

numerical model for heat transfer across the wall is described and the three virtual walls and boundary conditions provided.

2.1 The HFM Method According to the Standard

The in situ estimation of the thermal conductance is based on the monitoring of the indoor and outdoor surface temperatures (T_{si} and T_{se} respectively) of a given wall, along with the heat flux density (φ) at one of these surfaces. More precisely, the ISO 9869-1:2014 suggests sampling this quantity at the indoor surface, due to a generally greater stability.

Data processing is then performed according to two possible techniques, the Average Method (AM) and the Dynamic Method (DM).

The sampling period is suggested as being at least 72 h, but it can be longer if required. This parameter is subject of discussion later in this work. As far as sampling frequency is concerned, it can be around 0.5÷1 h for the AM, while for the DM no explicit indication is provided. However, in this work the sampling frequency is significantly increased, reducing the sampling interval to 5 minutes to allow more accurate estimations.

2.1.1 The Average Method

According to the AM approach, the overall thermal conductance Λ of the building envelope component is progressively evaluated while the measurement itself is ongoing, through the following equation:

$$\Lambda = \frac{\sum_{i=1}^{n} \varphi_i}{\sum_{i=1}^{n} \left(T_{si,i} - T_{se,i} \right)} \tag{1}$$

where φ_i, $T_{si,i}$, and $T_{se,i}$ are heat flux density [Wm⁻²], indoor and outdoor surface temperature [°C] respectively at the *i-th* sampling moment (with *i = 1÷N*). Both summations in Eq. 1 progress with time and their ratio should reach a stable value that approximates the real thermal conductance of the investigated component. This approach is based on the steady state assumption. For this reason, the standard suggests performing the sampling in winter periods, when outdoor conditions are more stable and larger heat flow densities usually occur. For elements with an expected thermal capacity lower than 20 kJ m⁻²K⁻¹), only data acquired during the nights should be used. The standard also provides three conditions for good estimation, i.e.:

- the test should last more than 72 h;
- the deviation between the result at the end of the test and the value reached 24 h before should be within ±5 %;
- the deviation between the results obtained considering the first 2/3 and the last 2/3 of the test duration should be within ±5 %.

In this work the constraint on the overall test duration is not strictly considered in order to investigate how much the sampling period can be reduced while maintaining an acceptable outcome of the procedure. At the same time, the other two conditions are always checked. Moreover, the standard suggests either the use of a thermal mass factor correction or the implementation of the DM whenever the change in internal energy of the wall is more than 5 % of the heat passing through the wall during the test. Since it is not clearly explained how this condition should be assessed and this work deals with the DM anyway, no thermal mass factor correction is considered.

2.1.2 The Dynamic Method

This second processing technique is suggested as a way of estimating the steady-state properties of a building element starting from highly variable temperatures and heat fluxes and is applied at the end of their acquisition. It is based on the solution of the Fourier equation through the Laplace transformation method (Ahvenainen et al., 1980):

$$\begin{aligned} \varphi_i = \ & \Lambda\left(T_{si,i} - T_{se,i} \right) + \\ & + K_1 T'_{si,i} - K_2 T'_{se,i} + \\ & + \sum_n P_n \sum_{j=i-p}^{i-1} T_{si,j} (1 - \beta_n) \beta_n (i - j) + \\ & + \sum_n Q_n \sum_{j=i-p}^{i-1} T_{se,j} (1 - \beta_n) \beta_n (i - j) \end{aligned} \tag{2}$$

where $T'_{si,i}$ and $T'_{se,i}$ are the surface temperature time derivatives [K s⁻¹] at the *i-th* sampling moment (approximated using the incremental ratio referred to the sampling interval Δt), K_1, K_2, P_n and Q_n are unknown dynamic characteristics of the wall that depend on the *n-th* time constant τ_n (also unknown). Even though the number of time constants should be theoretically infinite, a limited number *m* (generally from 1 to 3) is adequate to correctly describe the system behaviour. Finally, β_n is defined as:

$$\beta_n = e^{-\Delta t/\tau_n} \tag{3}$$

Once the m time constants are initialized, the ($2m+3$) unknowns are iteratively calculated optimizing the τ_n, through the minimisation of the square deviation between the measured and the estimated (φ^*_i) heat flux densities:

$$S^2 = \sum (\varphi_i - \varphi_i^*)^2 \tag{4}$$

The sums over the index j in Eq. 2 are the approximation of the integration process and are performed over a supplementary subset of p data, with $p = M-N$ and M the number of data triplets (φ_i, $T_{si,i}$, and $T_{se,i}$) that are actually used in the estimation of φ^*_i, as shown in Fig. 1.

Therefore, the user is expected to choose the number of time constants m (and their starting value for the iteration process) and M. While the standard provides some indications about the former, the latter is left to the user's experience (the only constraint is $M > 2m+3$). No univocal criterion is provided to assess the quality of the estimation and, ultimately, of the thermal conductance Λ achieved: the technical standard reports only an equation to calculate the confidence interval I for the estimated Λ (see ISO 9869-1:2014), stating that whenever I is lower than 5 % of the estimated conductance, the latter is generally close to the real value.

As far as the DM is concerned, this work aims at:

- assessing its effectiveness for different wall kinds, both in winter and summer conditions;
- evaluating the sensitivity of the outcomes on the number and the initial values of the time constants considered;
- evaluating the sensitivity of the method to the parameter M, possibly finding useful indications for the user.
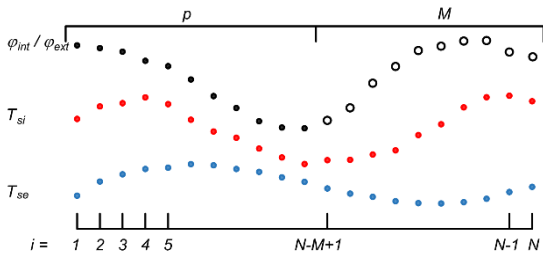
Fig. 1 – data utilization representation for the DM, with indication of p and M

2.2 The Numerical Model

In this work virtual experiments are performed using a one-dimensional Finite Difference model based on the one presented and validated in (Alongi et al., 2021). For a given k-th layer of the wall ($k = 1 \div K$), the discretized version of the Fourier equation is:

$$\frac{T_i^{j+1} - T_i^j}{\Delta t} = \alpha_k \frac{T_{i+1}^{j+1} - 2T_i^{j+1} + T_{i-1}^{j+1}}{\Delta x^2} \tag{5}$$

where α_k is the thermal diffusivity, T_i^j is the temperature at the i-th node ($i = 1 \div N_{FD}$) and at the j-th timestamp ($j = 1 \div M_{FD}$), Δx and Δt are the space and time discretization respectively. The numerical model uses a central difference scheme for the spatial derivative and a fully implicit representation of the time variation.

Third type boundary conditions are imposed at both edges of the domain, along with an imposed heat flux at the outdoor surface to take into account solar radiation, while temperature and heat flux continuity is imposed at the interface between adjacent layers. In all simulations performed, a structured grid is considered, with a constant step $\Delta x = 0.001$ m (which in (Alongi et al., 2021) is suggested as a good compromise between accuracy and computational cost), and the timestep Δt is set equal to 300 s.

The main outcomes of the simulations used by both the AM and the DM are the surface temperature trends, along with the corresponding heat flux densities. For the latter, the three-points formulation is chosen as in (Alongi et al., 2021):

$$\varphi_{ext}^j = -\lambda_1 \frac{3T_3^j - 4T_2^j + T_1^j}{2\Delta x} \tag{6}$$

$$\varphi_{int}^j = -\lambda_K \frac{3T_{N_{DF}}^j - 4T_{N_{DF}-1}^j + T_{N_{DF}-2}^j}{2\Delta x} \tag{7}$$

where φ_{ext} and φ_{int} are the heat flux densities at the outer and the inner edges of the domain, respectively, both positive when directed inward.

2.3 The Virtual Samples

The effectiveness of the two methods is evaluated on three walls with different thermophysical properties, used as virtual samples: a light and well insulated dry wall (W1); a heavy wall (W2); an externally insulated wall (W3). Layer sequences and material thermal properties are reported in Table 1 (density ρ, thermal conductivity λ, specific heat c and thickness s), along with the following reference quantities, calculated as follows:

- thermal conductance

$$\Lambda_{ref} = \left(\sum R_{cd,i} + \sum R_{cav,j}\right)^{-1} \qquad (8)$$

- Specific heat capacity per unit area

$$C_{ref} = \sum (\rho_i \cdot c_i \cdot s_i) \qquad (9)$$

- time constant

$$\tau_{ref} = \sum (R_{cd,i} \cdot C_i) \qquad (10)$$

where C_i [J·m^{-2} K^{-2}] and $R_{cd,i}$ [m^2 K·W^{-1}] are the heat capacity per unit surface and the conductive resistance, respectively, of the *i-th* solid layer, $R_{cav,j}$ is the convective-radiative resistance of the *j-th* gap. It can be noticed that for all the walls C$_{ref}$ is larger than 20 kJ m^{-2} K^{-1}.

Table 1 – names and main properties of the virtual samples

	ρ [kgm^{-3}]	λ [Wm^{-1}K^{-1}]	c [Jkg^{-1}K^{-1}]	s [m]
W1 - light and insulated wall				
sandwich	230	0.532	1500	0.04
rock wool	70	0.033	1030	0.2
air gap	-	-	-	0.055
rock wool	40	0.035	1030	0.04
Λ_{ref} = 0.134 Wm^{-2}K^{-1}		C$_{ref}$ = 30 kJm^{-2}K^{-1}		τ_{ref} = 0.54 d
W2 - heavy wall				
plaster	1800	0.9	1000	0.03
brick wall	1800	0.787	1000	0.425
plaster	1400	0.7	1000	0.02
Λ_{ref} = 1.661 Wm^{-2}K^{-1}		C$_{ref}$ = 847 kJm^{-2}K^{-1}		τ_{ref} = 5.00 d
W3 - externally insulated wall				
plaster	1300	0.3	840	0.03
rock wool	120	0.035	1030	0.06
hollow bricks	1000	0.163	1000	0.3
plaster	1400	0.7	1000	0.02
Λ_{ref} = 0.271 Wm^{-2}K^{-1}		C$_{ref}$ = 368 kJm^{-2}K^{-1}		τ_{ref} = 6.50 d
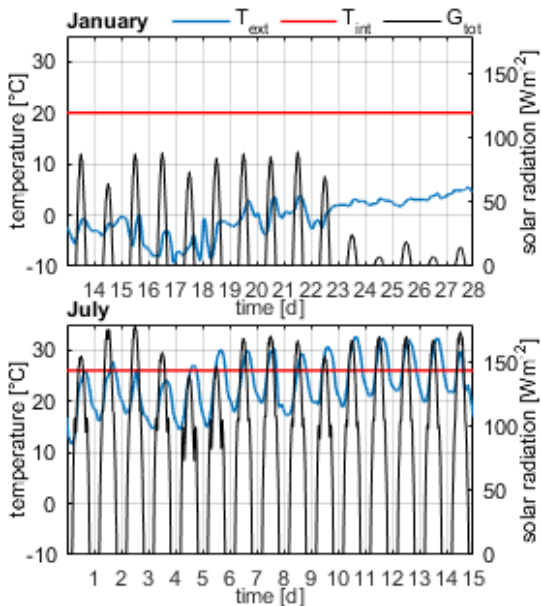
Fig. 2 – Indoor and outdoor boundary conditions for the two 14-day periods considered

As boundary conditions, two alternative indoor constant values for operative temperatures are considered: 20 °C in winter (from October 15th to April 15th) and 26 °C in summer (the rest of the year). Daily variations are neglected, limiting fluctuations to those caused by the outdoor conditions, which are based on the Typical Meteorological Year for Milan-Linate (Italy). More in detail, both external operative temperature and total solar radiation on a vertical surface facing North are used. Finally, even though the whole year is simulated, only the two most relevant 14-day periods are considered: from the 14th to the 28th of January for winter and from the 1st to the 15th of July for summer (Fig. 2).

3. Results And Discussion

The simulations provide the trends of the surface temperatures and the heat fluxes for each wall. For the sake of brevity, Fig. 3 shows only the results for W1 as an example, while Table 2 reports the main performance of each virtual sample (average, minimum and maximum for every quantity).

During the winter period, the three walls show stable thermal conditions, with indoor-outdoor temperature differences constant in sign. Heat flux densities, however, feature higher oscillations on the outer boundaries, with several sign inversions for all walls except W1. A more stable behavior can be observed on the indoor side (no sign inversions), with heat flux density always below 1 W m^{-2} for W1. Greater instability can be observed during the summer period, with multiple sign changes for both temperature difference and heat fluxes. These virtual measurements are then used to estimate Λ.

3.1 The Average Method Results

This method has been applied for each wall to the two complete 14-day periods, starting the average process at the beginning of each time window and considering the indoor and outdoor heat flux densities alternatively. Fig. 4 shows the conductance curves obtained in both periods for each wall investigated. The time needed to achieve a reliable estimation is actually the minimum time period
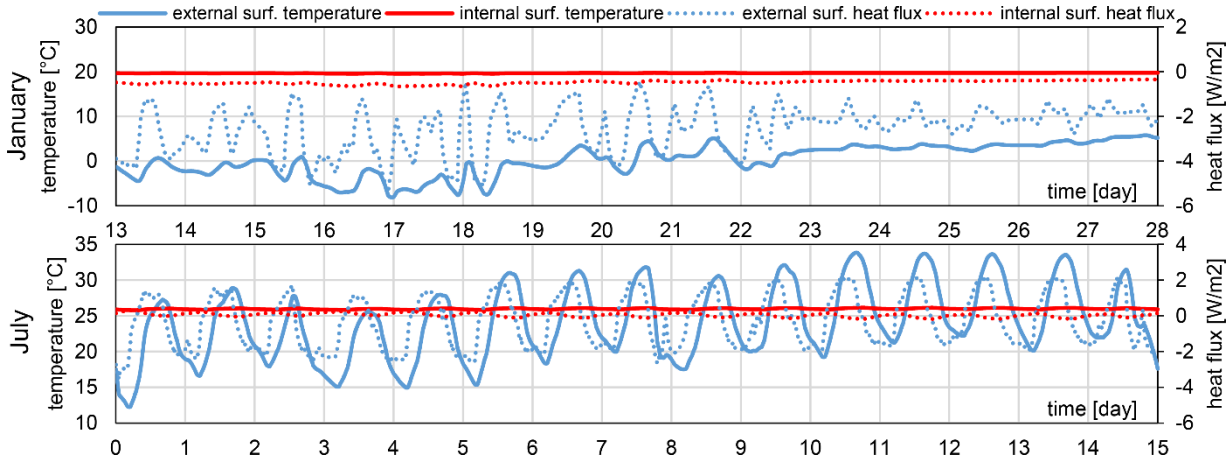
Fig. 3 – Simulation results (indoor and outdoor temperature and heat flux density fluctuations) for the W1 virtual sample

Table 2 – Average, minimum and maximum indoor and outdoor surface temperatures and heat flux densities for each virtual sample

		W1				W2				W3			
		T_{se} [°C]	T_{si} [°C]	φ_{ext} [Wm^{-2}]	φ_{int} [Wm^{-2}]	T_{se} [°C]	T_{si} [°C]	φ_{ext} [Wm^{-2}]	φ_{int} [Wm^{-2}]	T_{se} [°C]	T_{si} [°C]	φ_{ext} [Wm^{-2}]	φ_{int} [Wm^{-2}]
Jan.	av.	0.23	19.67	-2.55	-0.48	0.58	16.48	-25.15	-27.14	-0.23	19.29	-5.04	-5.49
Jan.	min	-8.15	19.54	-5.40	-0.66	-6.63	15.69	-79.90	-33.22	-8.79	19.16	-26.31	-6.45
Jan.	max	5.78	19.76	-0.45	-0.35	5.92	17.26	28.72	-21.10	5.48	19.42	24.54	-4.44
July	av	24.12	25.97	-0.30	0.04	24.13	25.64	-2.29	2.77	24.06	25.92	-0.47	0.60
July	min	12.23	25.78	-3.54	-0.18	14.31	25.01	-94.45	-2.26	12.05	25.83	-38.56	-0.24
July	max	33.84	26.12	2.18	0.32	32.26	26.29	63.20	7.66	33.90	26.03	27.15	1.32

required to fulfil the constraints provided by the ISO 9869-1:2014. The main results for each wall are reported in Table 3, where *n.a.* means that for a given condition it was not possible to satisfy the standard constraints within the 14-day period. It is possible to observe that acceptable outcomes (i.e., up to 5 % accuracy) can be achieved for every wall in the winter conditions minimum period required by the standard, provided that the proper heat flow density is chosen. In general, while both W2 and W3 feature acceptable outcomes with both heat flux densities, with an improvement when the indoor one is considered, for W1 only φ_{ext} provides accurate results, while φ_{int} leads to an unacceptable value of Λ. This is possibly due to the small values of the indoor heat flux density, as a consequence of the high insulation level. Table 3 also shows that increasing the evaluation period up to 14 days does not lead to a significant improvement, as the corresponding estimated conductance Λ_{14} shows.

As far as the summer conditions are concerned, the constraints of the standard are never met for W2 and W3, while 5 days are needed for W1. However, despite satisfying the constraints given by the ISO 9869-1:2014 for W1, estimations based on the indoor

heat flux density lead to an unacceptable value of the thermal conductance (-82 %), while with φ_{ext}, Λ never stabilizes around an asymptotic value (Fig. 3). This oscillatory trend is also present in W2 and W3, wherever the heat flux is measured. These analyses show that the indications provided by the standard are only partially effective: first of all, a stable heat flux is not enough to achieve a reliable estimate of the thermal conductance, but it needs to be above a threshold (even the -6 to -4 W m^{-2} observed for W3 seem to suffice); more reliable outcomes are achieved with highly insulated walls when φ_{ext} is used. Moreover, the constraints in the standard only deal with the apparent stability of the thermal conductance estimate and can be misleading in some cases, like what happens for W1 either considering φ_i in the winter period or both heat flux densities in the summer period. Thus, the calculations required by the standard must be supported by a critical evaluation of the outcome and a visual inspection of the thermal conductance trend during the whole period.

3.2 The Dynamic Method Results

The DM has been tested on each wall considering several time windows within the two simulated periods to evaluate the shorter time needed to achieve a reliable estimation. A first sensitivity analysis demonstrated that the number of time constant has little effect on the outcomes. Thus, only one time constant is considered ($m = 1$), to reduce computational costs. Fig. 5 shows the thermal conductance and the square deviation achieved with the shorter data set, among the several investigated, used for each wall and each climate, both as function of M. Moreover, conductance trends feature the confidence interval (coloured areas), calculated as indicated by the ISO 9869-1:2014.

Outcomes for W1 are similar to those achieved with the AM: despite the better stability, φ_{int} does not provide acceptable results, while better agreement between estimated and reference Λ is obtained using φ_{ext}. Moreover, winter conditions lead to more stable results, while summer ones show a great dependence on M. In both seasons two days are enough to achieve acceptable results (Table 3).

As far as W2 is concerned, better outcomes are achieved using the heat flux density at the indoor surface both in January and in July, with a greater stability observable in the winter period (Table 3), when two days of data are enough. Indeed, the summer period needs a three-day data set and leads to a trend with a great dependence on the M parameter and, therefore, is more difficult to interpret. Finally, W3 seems to be more difficult to investigate:

Table 3 – Main outcomes of the AM and the DM for the three virtual samples and the two periods investigated

| | | | W1 | | | | W2 | | | | W3 | | | |
| | | | January | | July | | January | | July | | January | | July | |
			int	ext	int	ext	int	ext	int	ext	int	ext	int	ext
AM		t	[d]	3	3	5	5	3	5	n.a.	n.a.	3	5	n.a.	n.a.
		Λ	[W/(m²K)]	0.024	0.139	0.024	0.145	1.609	1.826	n.a.	n.a.	0.258	0.305	n.a.	n.a.
		err.		-81.9%	3.7%	-82.0%	8.4%	-3.1%	10.0%	n.a.	n.a.	-4.5%	13.1%	n.a.	n.a.
		Λ_{14}	[W/(m²K)]	0.025	0.131	0.023	0.163	1.707	1.582	1.833	1.520	0.282	0.258	0.321	0.250
		err.	[%]	-81.7%	-2.0%	-82.5%	21.8%	2.8%	-4.7%	10.4%	-8.4%	4.3%	-4.4%	18.9%	-7.4%
DM	**best case**	t	[d]	2	2	2	2	2	2	3	3	3	3	6	6
		N	[-]	575	575	575	575	575	575	863	863	863	863	1727	1727
		Λ	[W/(m²K)]	0.029	0.134	0.027	0.133	1.663	1.656	1.518	2.057	0.259	0.271	0.227	0.350
		err.	[%]	-78.2%	0.0%	-79.8%	-0.5%	0.2%	-0.3%	-8.6%	23.9%	-4.2%	0.5%	-15.9%	29.6%
		τ_1	[d]	0.85	0.12	0.63	0.13	0.48	0.01	0.07	0.08	0.24	0.01	0.17	0.16
		M	[-]	86	466	76	446	296	326	786	796	726	736	1606	1636
	S² loc	Λ	[W/(m²K)]	0.025	0.136	0.025	0.133	1.620	1.746	1.499	2.234	0.254	0.285	0.227	0.455
		err.	[%]	-81.7%	1.3%	-81.6%	-0.5%	-2.4%	5.2%	-9.7%	34.6%	-5.8%	5.5%	-15.9%	68.6%
		M	[-]	416	536	436	446	506	526	796	816	806	846	1606	1456
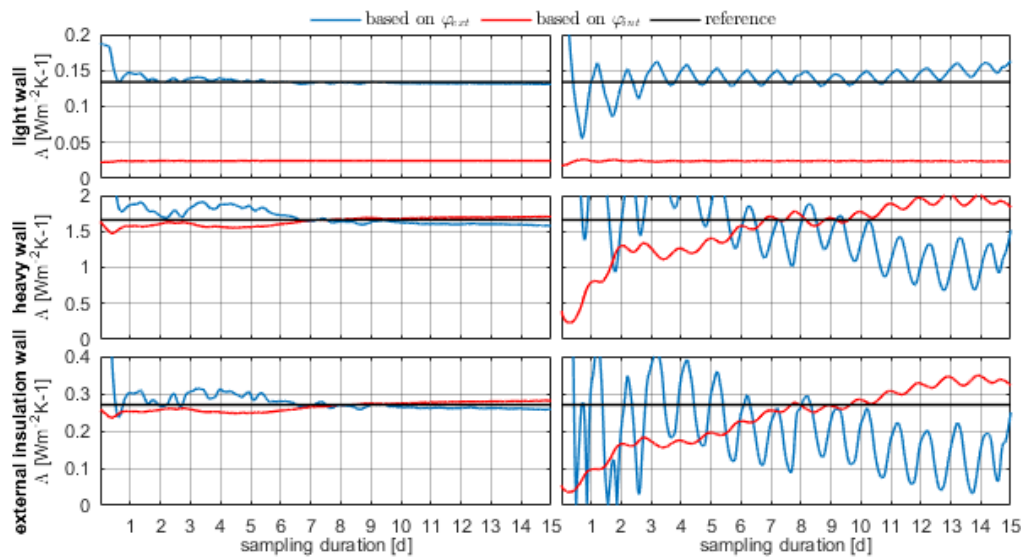
Fig. 4 – Outcomes of the AM: progressive estimate of Λ for the three walls in January and July, considering φ_{ext} and φ_{int}

three days of data are needed in winter to achieve an acceptable result, for both indoor and outdoor heat flux densities, while in summer several time frames have been considered (1 to 14 days) without success (the six-day one is shown in Fig. 5).

In general, the interpretation of the outcomes of each analysis is not straightforward: the sensitivity to M is great in several cases and the lack of clear indications by the ISO 9869-1:2014 may be an issue in a real implementation of this method, since the reference thermal conductance to validate the estimations is usually unknown. Moreover, the indication on the value of the confidence interval

mentioned previously does not provide any guidance: the fulfilment of this criterion, shown in Fig. 5 as horizontal coloured bars in the S^2 graphs, occurs for many values of M, even when the discrepancy between reference and estimated thermal conductance is unacceptable. Also, the post-fitting value of the time constant does not provide any indication about the reliability of the results: τ_1 in the best conductance estimates shown in Table 3 (grouped under *best case*) differs significantly from the respective lumped capacity reference τ_{ref} (Eq. 10), suggesting that it is not possible to assign this physical meaning to τ_1.
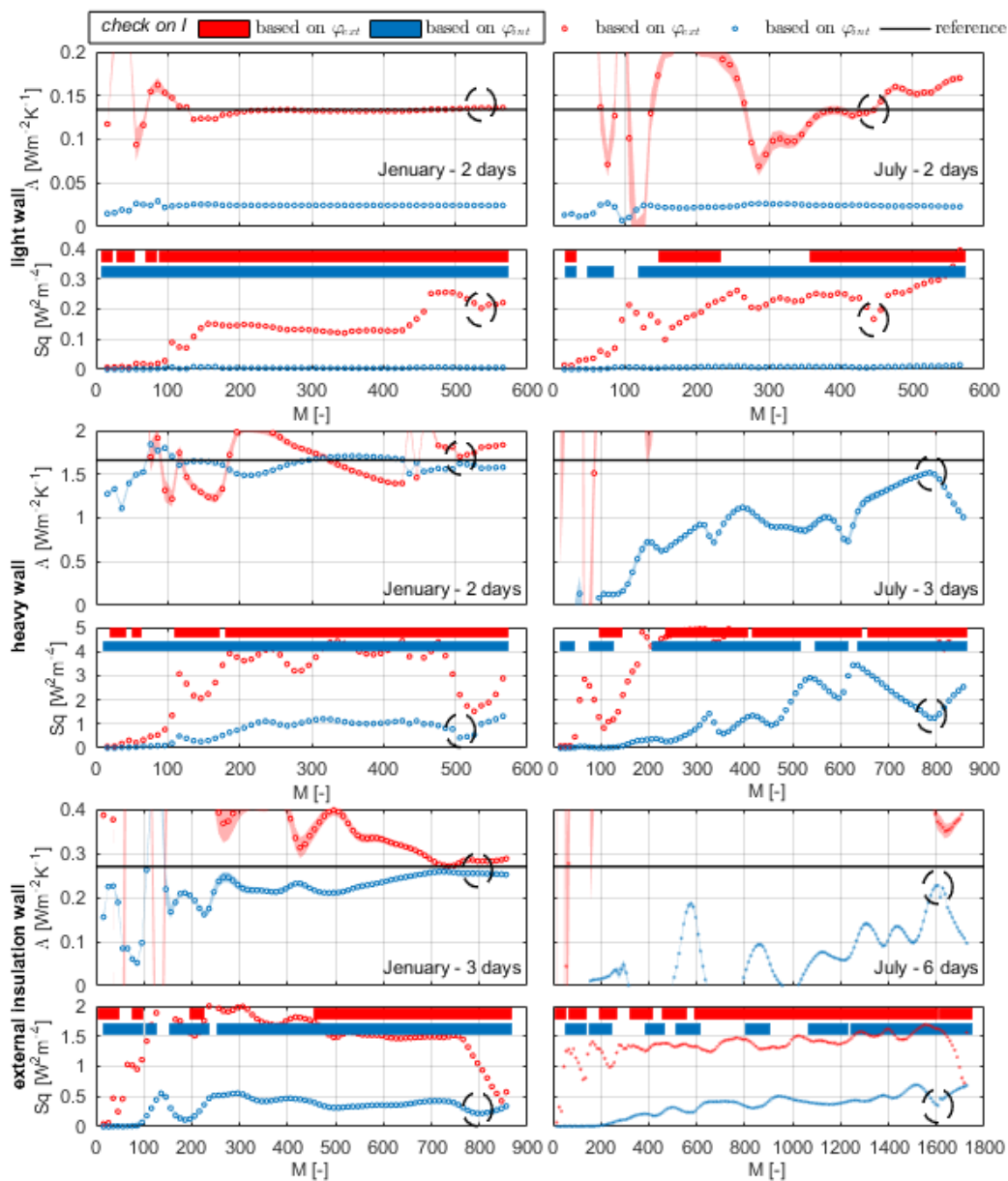
Fig. 5 – Outcomes of the DM: estimate of Λ and S^2 as function of M for the three walls in January and July, considering φ_{ext} and φ_{int}

Andrea Alongi, Luca Sala, Adriana Angelotti, Livio Mazzarella

To identify the most accurate estimate of Λ, a possible indication might come from the S^2 trend as function of M: good outcomes are indeed achieved for values of M greater than $N/2$ and corresponding to the last local minimum of S^2 (highlighted by dashed circles in Fig. 5 and grouped in Table 3 as S^2 *loc min*). This behaviour has been observed in several other cases, when different time frames have been considered. Therefore, it suggests that a technician should perform a sensitivity analysis on M and evaluate the outcomes using the S^2 trend as described above. Yet, this observation only suggests a possible line of investigation: this approach will need further analyses to provide a mathematical explanation and verify its repeatability.

4. Conclusions

This work investigates the accuracy of the post processing techniques provided by the ISO 9869-1:2014 by means of numerical simulations on three virtual wall samples, and focuses on two 14-day periods in January and July.

The analyses on the AM show that the best period to implement this technique is winter, in agreement with the standard. However, even though the latter suggests considering the heat flux density at the surface where it is more stable, it has been proven that a proper amplitude of the signal is more important than stability when dealing with highly insulated walls. Moreover, the criteria included in the standard can be misleading at times, as observed for W1, either in summer or, if φ_{int} is considered, in winter. Thus, a careful analysis of the conductance trend with time is needed to verify convergence to a stable and reasonable value.

As far as the DM is concerned, it generally leads to acceptable outcomes with acquisition periods shorter than the AM in winter, and summer measurements can be used too. W1 shows the same behavior described above, providing acceptable Λ only when the outdoor heat flux is considered in both periods. Results for both W2 and W3 are less sensitive to the choice between φ_{int} and φ_{ext} in winter, while in summer only the indoor one is useful for W2 and no reasonable outcome is obtained for W3 for every timespan considered. Dealing now with

the parameters of the method, while the number and the initial values of the time constants do not affect the final outcomes, great sensitivity on M is observed, which makes the results difficult to interpret when the method is applied, as expected, to a wall with unknown properties.

However, there is a correspondence between an acceptable thermal conductance value and the local minimum of the S^2 for M near to N. This finding will need further investigations in order for it to be confirmed and formally systematized.

References

Ahvenainen, S., E. Kokko, and A. Aittomaki. 1980. "Thermal conductance of wall-structures" Report 54. Espoo: Technical Research Centre of Finland, Laboratory of Heating and Ventilating.

Alongi, A., A. Angelotti, and L. Mazzarella. 2021. "A numerical model to simulate the dynamic performance of Breathing Walls". *Journal of Building Performance Simulation* 14 (2): 155-180. doi: https://doi.org/10.1080/19401493.2020.1868578

Atsonios, I. A., I. D. Mandilaras, D. A. Kontogeorgos, and M. A. Founti. 2017. "A comparative assessment of the standardized methods for the in-situ measurement of the thermal resistance of building walls." *Energy and Buildings* 154: 198-206. doi: https://doi.org/10.1016/j.enbuild.2017.08.064

Gaspar, K., M. Casals, and M. Gangolells. 2018. "In situ measurement of façades with a low U-value: avoiding deviations." *Energy and Buildings* 170: 61–73. doi: https://doi.org/10.1016/j.enbuild.2018.04.012

International Standard. 2014. ISO 9869-1:2014 - Thermal insulation — Building elements — In-situ measurement of thermal resistance and thermal transmittance — Part 1: Heat flow meter method.

Lucchi, E. 2017. "Thermal transmittance of historical stone masonries: a comparison among standard, calculated and measured data." *Energy and Buildings* 151: 393–405. doi: https://doi.org/10.1016/j.enbuild.2017.07.002